

ANRCP-1998-9
August 1998

Amarillo National Resource Center for Plutonium

A Higher Education Consortium of The Texas A&M University System,
Texas Tech University, and The University of Texas System

REF
SEP 19 1998
OSTI

Criticality Analysis of Selected Saxton Plutonium Program Experiments Using WIMS-D4M and DIF3D

Gabriel F. Cuevas Vivas and Theodore A. Parish
Department of Nuclear Engineering
Texas A&M University

This report was prepared with the support of the U.S. Department of Energy (DOE), Cooperative Agreement No. DE-FC04-95AL85832. However, any opinions, findings, conclusions, or recommendations expressed herein are those of the author(s) and do not necessarily reflect the views of DOE. This work was conducted through the Amarillo National Resource Center for Plutonium.

MASTER

DISTRIBUTION OF THIS DOCUMENT IS UNLIMITED

Edited by

Angela L. Woods
Technical Editor

600 South Tyler • Suite 800 • Amarillo, TX 79101
(806) 376-5533 • Fax: (806) 376-5561
<http://www.pu.org>

DISCLAIMER

This report was prepared as an account of work sponsored by an agency of the United States Government. Neither the United States Government nor any agency thereof, nor any of their employees, makes any warranty, express or implied, or assumes any legal liability or responsibility for the accuracy, completeness, or usefulness of any information, apparatus, product, or process disclosed, or represents that its use would not infringe privately owned rights. Reference herein to any specific commercial product, process, or service by trade name, trademark, manufacturer, or otherwise does not necessarily constitute or imply its endorsement, recommendation, or favoring by the United States Government or any agency thereof. The views and opinions of authors expressed herein do not necessarily state or reflect those of the United States Government or any agency thereof.

DISCLAIMER

**Portions of this document may be illegible
in electronic image products. Images are
produced from the best available original
document.**

AMARILLO NATIONAL RESOURCE CENTER FOR PLUTONIUM/
A HIGHER EDUCATION CONSORTIUM

A Report on

**Criticality Analysis of Selected Saxton Plutonium Program Experiments Using WIMS-D4M
and DIF3D**

Gabriel F. Cuevas Vivas and Theodore A. Parish
Department of Nuclear Engineering
Texas A&M University
College Station, Texas 77840

Submitted for publication to

Amarillo National Resource Center for Plutonium

August 1998

Criticality Analysis of Some of the Saxton Plutonium Program Experiments Using WIMS-D4M and DIF3D

Gabriel F. Cuevas Vivas and Theodore A. Parish

Department of Nuclear Engineering

Texas A&M University

College Station, Texas 77840

Abstract

The Saxton critical experiments were simulated with homogenized region, multigroup cross sections from the WIMS-D4M lattice physics code (ENDF/B-V library) and the diffusion code, DIF3D. The simulations were focused on assessing the codes' capabilities, including the different cell models available in WIMS-D4M. The accuracy of the core power distributions obtained with DIF3D has also been assessed. The number of experiments and their variety was used to obtain statistical parameters that allow a quantitative discussion of the assessment of the methodology.

TABLE OF CONTENTS

1. Introduction.....	1
2. Lattice Physics Analysis Code: WIMS-D4M	1
2.1 Regional Homogenization Model.....	1
3. DIF3D Core Calculations.....	7
4. SAXTON Program Experiments	7
4.1 Criticality Evaluations of the SAXTON Program Experiments.....	10
4.2 Analysis of the Effective Neutron Multiplication Factors.....	16
4.3 Power Distributions	18
5. Conclusions	27
References.....	29

LIST OF TABLES

Table 1: Seven Energy Group Partition for WIMS-D4M9	5
Table 2: Fuel Type Characteristics	8
Table 3: Classification of the SAXTON Criticals	10
Table 4: Saxton Critical Experiments (Single Region Analyses)	12
Table 5: Saxton Critical Experiments (Multiregion Analyses).....	14
Table 6: Void Effects on Plutonium Critical Experiments	15
Table 7: Analysis of Calculated K-effectives	17

LIST OF FIGURES

Figure 1: WIMS-D4M Cell Models.....	2
Figure 2: Spectra Comparison of PINCELL and SUPERCELL Models	3
Figure 3: Fission Cross Section of Uranium Fuel.....	4
Figure 4: Fission Cross Section of MOX Fuel.....	5
Figure 5: Typical Dimensions of a Multiregion Core	8
Figure 6: Examples of Saxton Core Configurations	9
Figure 7: Multiplication Factor as a Function of Fuel Rod Pitch	18
Figure 8: MOX Core with Water Slot.....	20
Figure 9: MOX Core with Aluminum Plate	21
Figure 10: Multi-region Core: 19x19 Fuel Rods, MOX Fuel Interior (11x11 Rods)	22
Figure 11: Multi-region Core: 19x19 Fuel Rods, Uranium Fuel Interior (11x11 Rods)	23
Figure 12: Multi-region Core: 27x27 Fuel Rods, MOX Fuel Interior (19x19 Rods), 1453 ppm B.....	24
Figure 13: Multi-region Core: 27x27 Fuel Rods, Uranium Fuel Interior (19x19 Rods), 1252 ppm B.....	25

1. INTRODUCTION

The criticality experiments performed under the SAXTON Plutonium Program have been simulated with the diffusion code, DIF3D, using its two-dimensional mode. The criticality of the experimental reactor cores were evaluated for different configurations (presence of one or two fuel types, void tubes, aluminum plate, control rods, boron), temperatures, and water heights. The simulations with DIF3D were carried out using multigroup, region average cross sections obtained from the lattice physics analysis code, WIMS-D4M, that employed an ENDF/B-V based nuclear data library.

Sixty-five experiments were selected for analysis based on the best information available from Taylor (1965). The experiments were classified into three major divisions:

- Single Region (either UO₂ or MOX).
- Multiregion (both fuels loaded the core).
- Void Effects on Plutonium Critical Experiments (MOX with void region).

The effective neutron multiplication factors for each configuration are presented in this report. This information was utilized to evaluate the codes' overall capabilities and accuracy for modeling these experiments. Power distributions for different configurations were also compared with experimental data. The core configurations are not presented in this report. Only summaries of the main characteristics are included here since there is no intention to replace the thorough descriptions that are provided in the main report (Taylor, 1996; Radulescu and Carron, 1997).

2. LATTICE PHYSICS ANALYSIS CODE: WIMS-D4M

WIMS-D4M is a transport code that calculates the neutron flux as a function of energy and space within one dimensional or simulated two dimensional cells. The code employs a fine group (69) nuclear data library derived from ENDF/B-V and it produces region average, broad group (up to 20) macroscopic cross sections for each composition (homogenized region) of the unit cell. This information is written in a binary file (ISOTXS) with a suitable format for later use in DIF3D.

2.1 Regional Homogenization Models

To execute the WIMS-D4M jobs, the DSN main transport solver was selected since its WIMS-D4M implementation allows more control on the accuracy of the flux solution. It usually is employed for larger unit cells than PERSEUS transport solution (collision probability) and is less expensive computationally (Deen, Woodruff, and Costescu, 1995).

The selection of the cell model used for homogenizing various core regions was of paramount importance. The cell model can be selected from the following:

PINCELL: A unit formed with a fuel rod (or pin) and its associated clad and coolant/moderator. This model assumes that the cell forms an infinite lattice of similar pincells.

MULTICELL: This cell is composed of two or more pincells and requires that the probability that neutrons can travel from one cell to another must be specified.

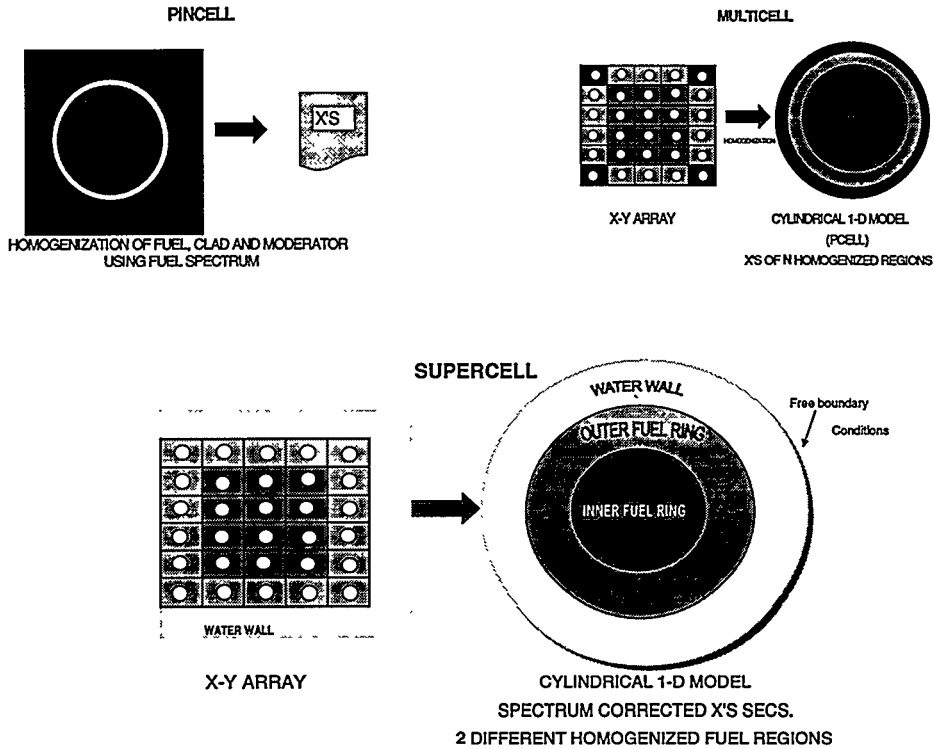


Figure 1: WIMS-D4M Cell Models

These probabilities are required as input because WIMS-D4M does not have a fully implemented two-dimensional collision probability transport module. The calculations of these probabilities are not straightforward. In general, the probabilities are approximated according to the number of neighbors of a specific type. However, this model proved to be very useful for most of the cores even when used to obtain perturbing element cross sections.

SUPERCELL: This type of cell is a rod cluster surrounded by the moderator and it can account for the softening of the neutron spectrum around rods near or in the outer row(s) of the cluster. The SUPERCELL is designed to provide properly

homogenized and resonance-corrected cross sections for subsequent use in more complex geometry, and support the treatment of multiple resonance materials (Deen, Woodruff, Costescu, 1995). For reactors with tight lattices (large fuel radius to rod pitch) this model could be used to represent the whole core and its surrounding water. Free boundary conditions (vacuum) are employed on the outer edge of such a SUPERCELL.

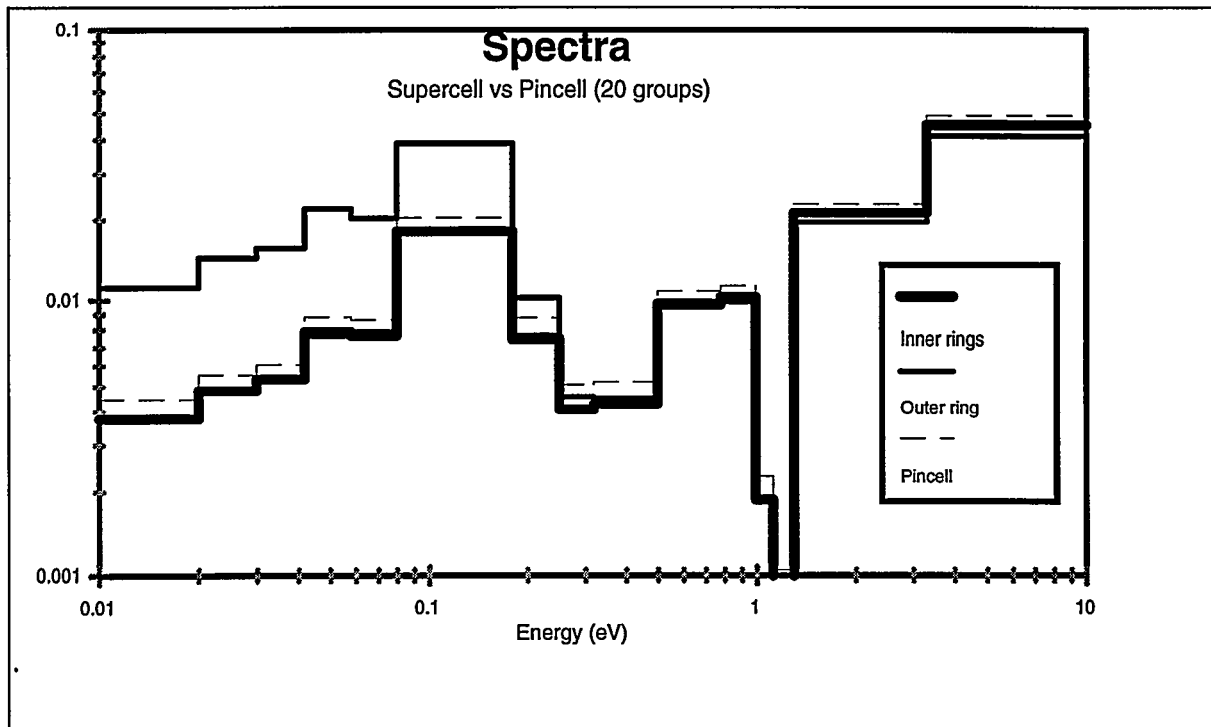


Figure 2: Spectra Comparison of PINCELL and SUPERCELL Model

In the analysis of the Saxton critical experiments, the SUPERCELL model was employed for most of the cases. When an experimental configuration included a heterogeneity, such as the presence of control rods, aluminum plates or void tubes, the cross sections for the heterogeneous region were calculated with a MULTICELL model and then incorporated in the ISOTXS nuclear data file to complete the set of cross sections for

the experimental core configuration.

Figure 1 illustrates each of the cell options available in WIMS-D4M. Note that the MULTICELL model may have many different fuel regions, but the SUPERCELL model only allows two different fuel regions. Therefore, the fuel regions employed in a SUPERCELL case were grouped to represent an outer fuel ring (fuel rods exposed to more moderation) and the inner fuel rings.

Figure 2 presents the spectra from a PINCELL and a SUPERCELL for a MOX core with a regular fuel rod pitch (1.4224 cm). The spectra calculations are depicted using a twenty flux group partition to highlight the relative differences of each spectrum. The PINCELL spectrum can be seen to be “harder” than the spectrum from the

SUPERCELL for the external fuel ring but slightly “softer” than the spectrum from the SUPERCELL for the inner fuel rings. Note the flux depressions around 0.2 and 0.5 eV and slightly above 1eV which correspond to absorption resonances due to Pu-239 and Pu-241, and Pu-240, respectively.

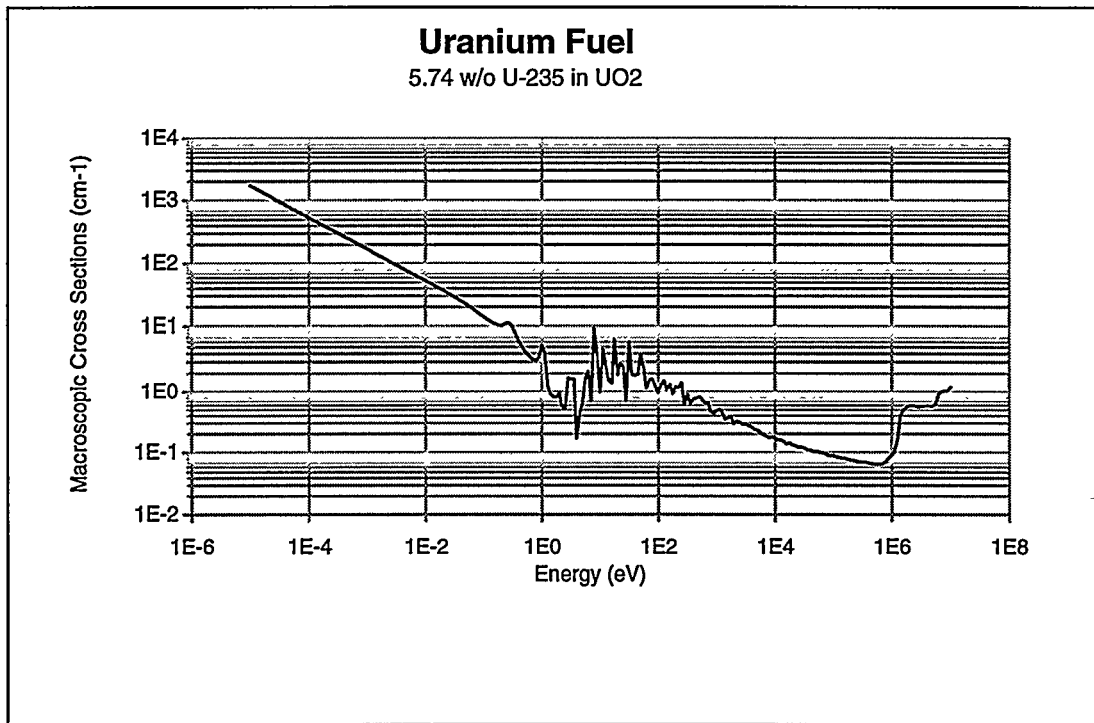


Figure 3: Fission Cross Section of Uranium Fuel

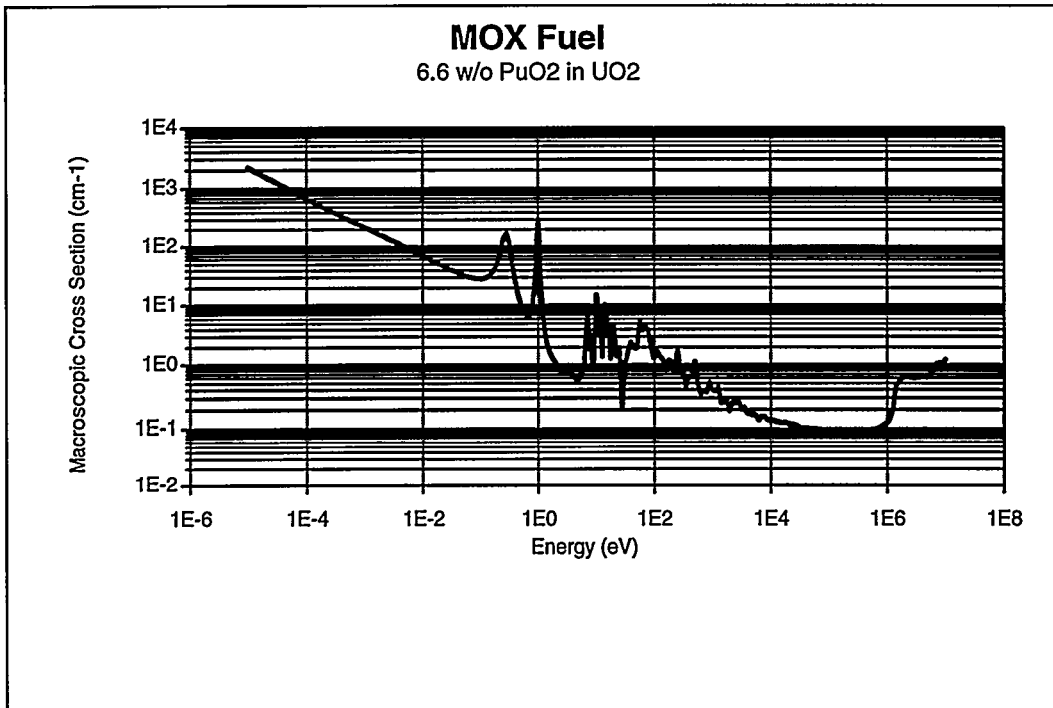


Figure 4: Fission Cross Section of MOX Fuel

Table 1: Seven Energy Group Partition for WIMS-D4M

Group	Energy Bounds (eV)
1	$\sim 10^7$ - 9118.0
2	9118.0 - 4.00
3	4.00 - 1.071
4	1.071 - 0.78
5	0.78 - 0.18
6	0.18 - 0.058
7	0.058 - 0.005

To complete the WIMS-D4M model, a suitable energy group partition had to be selected based on the energies of the resonance cross sections of the two fuel types (see Figures 3 and 4). The energy group partition employed to collapse the 69 group cross section data is shown in Table 1. This partition was selected to incorporate the

resonance cross sections of the fuel mixture into individual broad energy groups.

3. DIF3D CORE CALCULATIONS

DIF3D is a diffusion, finite difference, multigroup code utilized to evaluate the criticality of reactor cores and to determine the neutron flux distribution. It is designed to handle more than two energy groups and has a k-effective convergence scheme that is well suited to study fast reactors (Derstine, 1984). It utilizes improved numerical methodology which helps in obtaining three dimensional flux distributions in cores. However, the computer time still represents a strong limitation, especially when many energy groups are employed and the mesh size needs to be small. This is the case for the SAXTON Critical Experiments which were evaluated only in a 2D configuration using the critical water height to account for the axial leakage.

4. SAXTON PROGRAM EXPERIMENTS

This program, performed between March and June 1965, represents the first time that plutonium fuel was utilized in a commercial-licensed facility (Westinghouse Reactor Evaluation Center) and criticality was controlled mainly with the water inventory. Fuel type characteristics are summarized in Table 2, and a more thorough description, is presented in Taylor (1995) and Radelescu, Carron (1997). The experiments are mainly classified as being Single Region (one type of fuel), multi-region (uranium and plutonium fuels present) and Void Effect plutonium criticals. A more detailed classification of the experiments is presented in Table 3. Note that a significant number of experiments were performed with a fuel rod pitch of 1.4224 cm which provides a rod-pitch-to-pellet-diameter ratio near to the typical value of a commercial PWR assembly (~1.5). The multiplication factor and main characteristics of each experiments are presented in Tables 4, 5, and 6.

Table 2: Fuel Type Characteristics

Fuel Type	Enrichment	Density	Geometry	Clad Material
Uranium Dioxide	5.74 w/o U-235 in Uranium	Theoretical: 10.96 g/cm ³ (93% of Theoretical Density)	Pellet Diameter = 0.9067 cm Clad I.D. = 0.91694 cm Clad O.D. = 0.99314 cm Rod Length = 92.964 cm	304 SS
MOX	6.6 w/o PuO ₂ in UO ₂ Pu components: Pu-239 (90.49%) Pu-240 (8.57 %) Pu-241 (0.89 %) Pu-242 (0.04 %)	Theoretical: 11.46 g/cm ³ (94% of Theoretical Density)	Pellet Diameter = 0.8569 cm Clad I.D. = 0.87503 cm Clad O.D. = 0.99314 cm Rod Length = 92.964 cm	Zircaloy 4

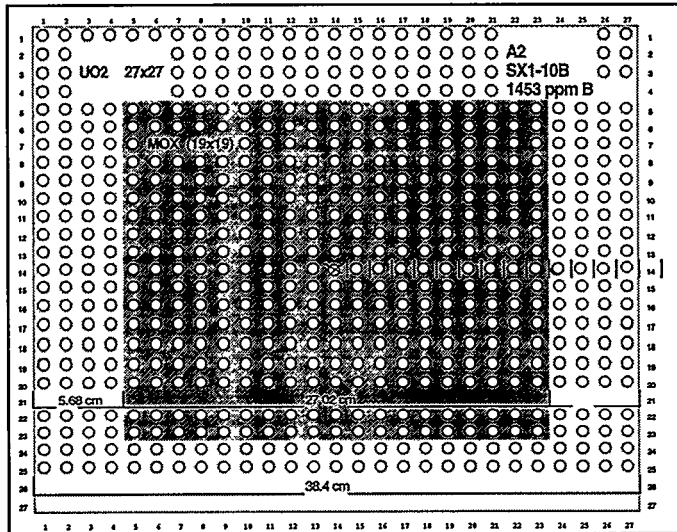


Figure 5: Typical Dimensions of a Multiregion Core

The locations of criticality perturbing elements such as an aluminum plate, water

slot and control rods (Ag-In-Cd, 80-15-5%) are generally in the center of the critical

assembly occupying the space left by five fuel rods. However, there are other cases when the perturbing element and/or different fuel regions are offset or located along the boundary of two fuel types (refer to Taylor

1995 for core layout). Figure 5 shows a sample of a typical core dimensions for a multiregion core and Figure 6 shows some examples of core configurations.

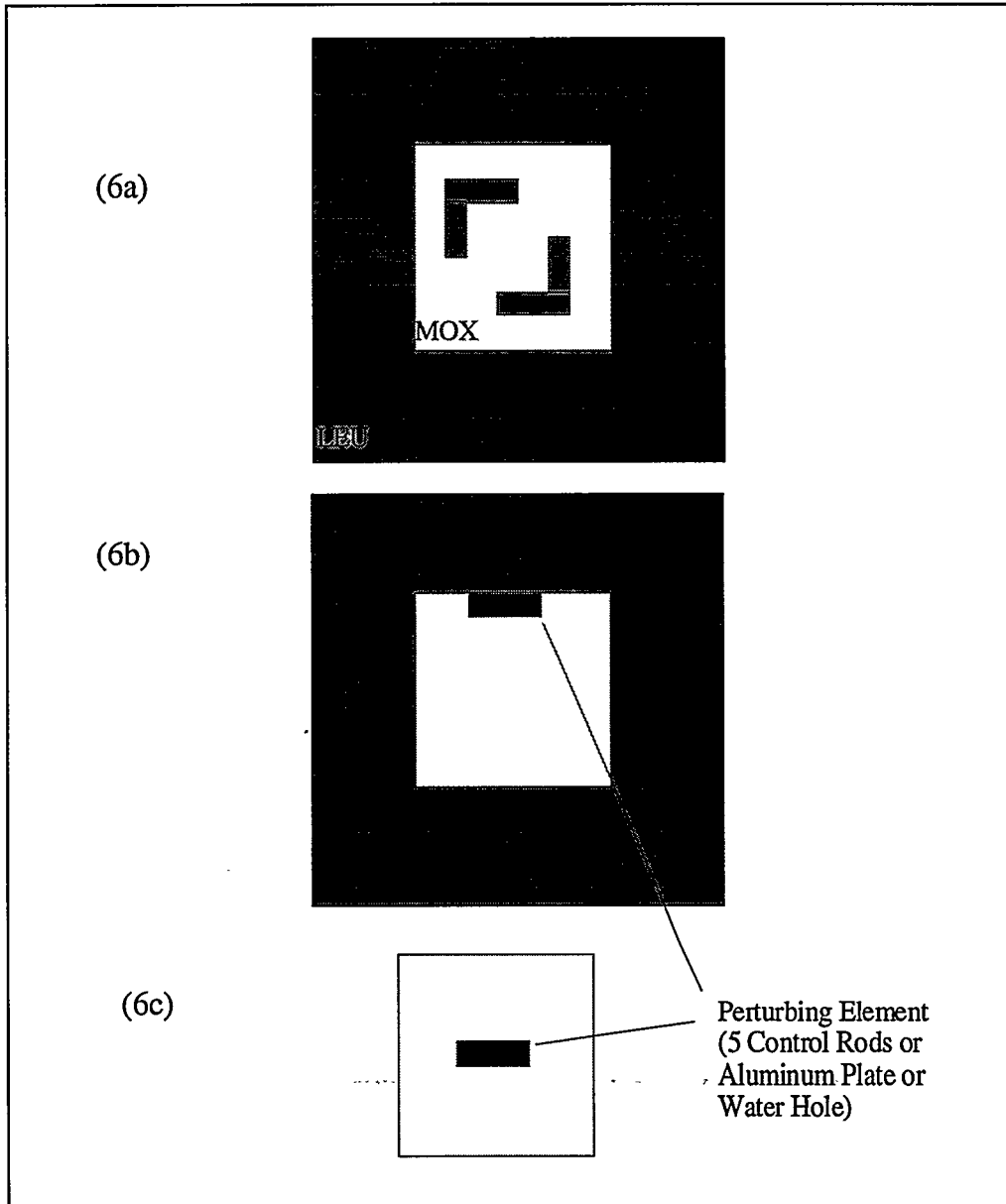
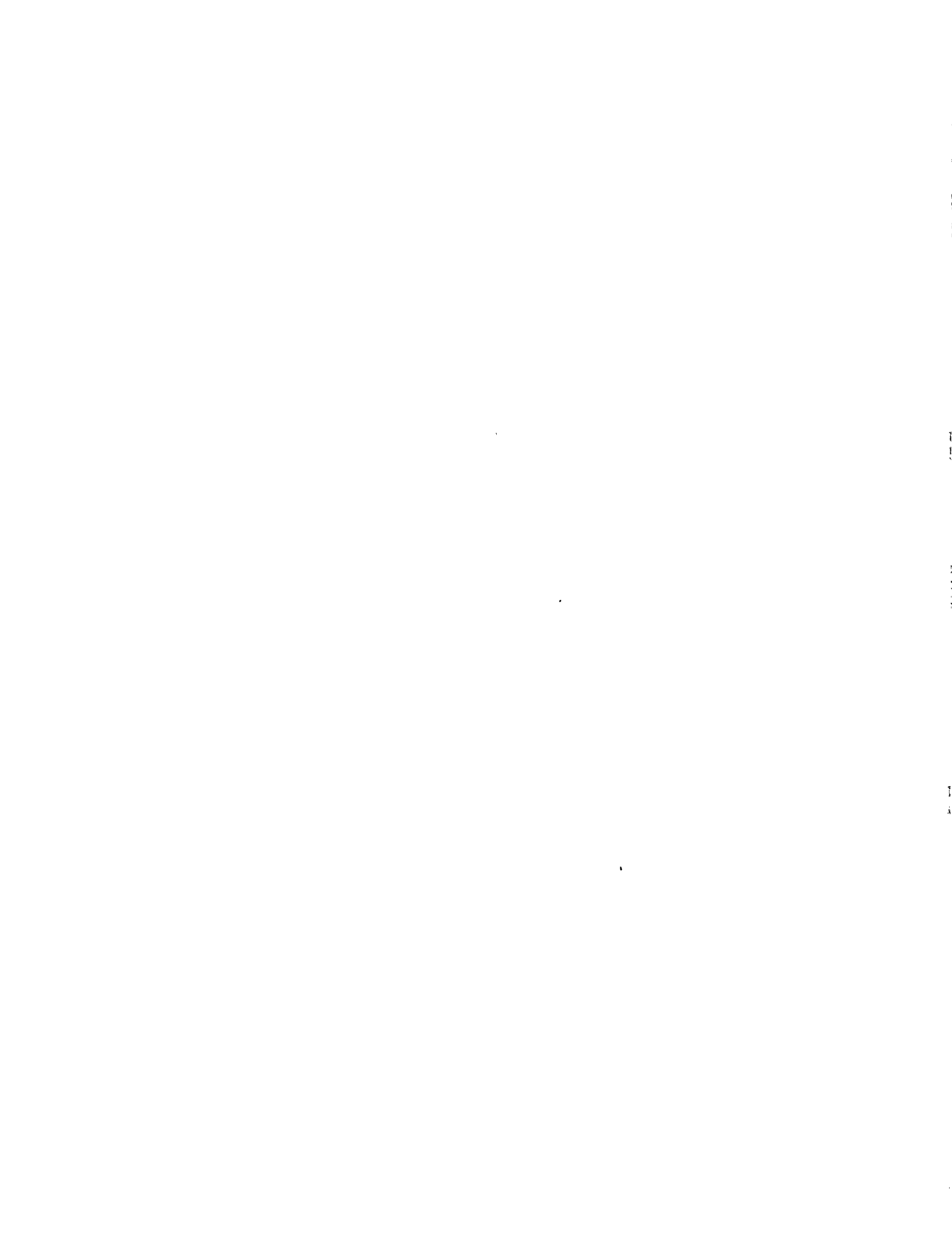


Figure 6: Examples of Saxton Core Configurations

(6a) Multiregion core with a L-shaped array of LEU fuel rods immersed in an internal square array of MOX fuel rods; (6b) Multiregion core showing the off-set location of a perturbing element; (6c) Single Region Core with a centered location of perturbing elements.



4.1 Criticality Evaluations of the SAXTON Program Experiments

Tables 4, 5, and 6 present a summary of the results from the criticality calculations

of 65 experiments, grouped in three divisions, and obtained using the codes WIMS-D4M and DIF3D (2D mode).

Table 3: Classification of the SAXTON Criticals

Classification	Configuration	Fuel type	No. of experiments
Fuel rod pitch	1.3208 cm.	Both	20
	1.4224 cm.	Both	37
	1.8669 cm.	PuO ₂ -UO ₂	2
	2.0117 cm.	Both	4
	2.6416 cm.	PuO ₂ -UO ₂	2
Cylindrical core		UO ₂	4
		PuO ₂ -UO ₂	5
Square core	11x11	PuO ₂ -UO ₂	1
	12x12	PuO ₂ -UO ₂	1
	13x13	PuO ₂ -UO ₂	1
	19x19	Both	15
	21x21	Both	8
	23x23	PuO ₂ -UO ₂	7
	27x27	Both	6
Rectangular core	13x14	UO ₂	1
	22x23	PuO ₂ -UO ₂	1
	25x23	PuO ₂ -UO ₂	3
Clean core	25x24	PuO ₂ -UO ₂	4
		UO ₂	6
		PuO ₂ -UO ₂	13
		Multiregion	4
Borated core		UO ₂	0
		PuO ₂ -UO ₂	6
		Multiregion	7
Criticality perturbing elements	Water slot	UO ₂	1
		PuO ₂ -UO ₂	1
		Multiregion	1
	Aluminum plate	UO ₂	1
		PuO ₂ -UO ₂	1

		Multiregion	2
Control rods (Ag-In-Cd)	UO ₂	1	
	PuO ₂ -UO ₂	1	
	Multiregion	1	
2 Void tubes surrounding a fuel rod	PuO ₂ -UO ₂	4	
4 Void Tubes surrounding a fuel rod	PuO ₂ -UO ₂	9	

Table 3 (con't)

Table 4: Saxton Critical Experiments (Single Region Analyses)

Fuel	Lattice pitch (cm)	Temp. (°K)	Core configuration	Critical height (cm)	Features	Case Number	K_eff (2D)	Comments
UO ₂	1.3208	290.75	Cylin.	92.964	447 rods	CR1	8A	0.988276
	1.4224	290.45	Cylin.	92.964	339 rods	CR2	6A	0.990177
	2.0117	290.45	Cylin.	92.964	173 rods	CR3	7A	0.995437
	1.3208	297.15	Cylin.	92.964	472 rods	CR4	3A	0.996983
	1.4224	290.65	Cylin.	92.964	337 rods	CR5	1A	1.001389
	1.8669	301.15	Cylin.	92.964	151 rods	CR6	4A	1.009652
	2.0117	290.15	Cylin.	92.964	133 rods	CR7	2A	1.010038
	2.6416	293.15	Cylin.	92.964	117 rods	CR8	5A	x
PuO ₂ -UO ₂	1.3208	292.35	Cylin.	93.630	449 rods	BU1	8B	0.992967
	1.4224	291.15	19x19	83.710		BU2	6B	0.999193
	2.0117	290.45	13x14	88.960		BU3	7B	1.001271
	1.3208	298.95	22x23	84.560		BU4	3B	1.008095
	1.4224	290.15	19x19	80.800		BU5	1B1	1.001792
	1.4224	288.90	19x19	83.450			1B2	1.002489
	1.4224	291.15	21x21	88.700		BU6	1N	1.010336
	1.8669	297.25	13x13	70.110	Boron: 337 ppm	BU7	4B	1.019590
UO ₂	2.0117	289.25	12x12	78.430		BU8	2B	1.018905
	2.6416	293.05	11x11	81.170		BU9	5B	1.023851
	1.4224	291.55	19x19	80.00				
	1.4224	291.55	19x19	83.60	w/ Water Slot @ (Unperturbed case)	PO1	6D	0.991759
	1.4224	291.15	19x19	87.38	w/ Al Plate @ (Unperturbed case)	UP01-6DE	0.990267	
	1.4224	291.55	21x21	83.60	w/ Ag-In-Cd @ (Unperturbed case)	PO3	6E	0.986826
	1.4224	291.15	21x21	89.02	w/ Ag-In-Cd @ (Unperturbed case)	UP03-6DE	0.992231	
	1.4224	289.25	21x21	52.66	w/ Water Slot @ (Unperturbed case)	PO5	6F	0.978745
PuO ₂ -UO ₂	1.4224	288.55	19x19	75.90	w/ Water Slot @ (Unperturbed case)	UP05-6FU	0.976889	
	1.4224	290.15	19x19	82.41	w/ Al Plate @ (Unperturbed case)	PO2	1D	1.002480
	1.4224	289.15	19x19	83.02	w/ Al Plate @ (Unperturbed case)	UP02-1D	1.001603	
	1.4224	290.15	21x21	82.41	w/ Ag-In-Cd @ (Unperturbed case)	PO4	1E	0.997141
	1.4224	288.55	21x21	79.01	w/ Ag-In-Cd @ (Unperturbed case)	UP04-1E	1.0033802	
						PO6	1F	0.989780

	1.4224	288.55		52.04		(Unperturbed case)		UPO6-1F	0.983940	
Fuel	Lattice pitch (cm)	Temp. (oK)	Core configuration	Critical height (cm)	Features		Case Number	K_eff (2D)	Comments	
PuO ₂ -UO ₂	1.4224	290.05	19x19	83.000	Borated Water		1L1	0.994295		
	1.4224	290.05	19x19	89.410			RW7 1L2	0.995188		
	1.4224	290.05	19x19	99.440			RW8 1L3	0.997279		
	1.4224	288.55	21x21	52.130	Borated Water		1M1	0.984555		
	1.4224	291.15	21x21	72.470			RW9 1M2	0.998995		
	1.4224	291.15	21x21	84.660			RW10 1M3	1.002856		
	1.4224	291.15	21x21	89.700			RW11 1M4	1.003685		

Table 4 (con't)

Table 5: Saxton Critical Experiments (Multi-region Analyses)

External fuel config.	Internal fuel config.	Lattice pitch (cm)	Temperature (°K)	Critical height (cm)	Additional feature	Boron conc. (ppm)	Case Number	K_eff (2D)	Comments
UO ₂ 19x19	PuO ₂ -UO ₂ 11x11	1.4224	289.35	91.070		0	A1-9B	0.993475	
UO ₂ 27x27	PuO ₂ -UO ₂ 19x19	1.4224	291.35	93.350		1453	A2-10B	0.998208	
UO ₂ 27x27	PuO ₂ -UO ₂ 19x19	1.4224	291.65	89.140	UO ₂ 3x3 @ Center	1425	A3-10F	0.996087	
PuO ₂ -UO ₂ 19x19	UO ₂ 11x11	1.4224	288.75	76.111		0	A4-11B	0.995835	
PuO ₂ -UO ₂ 27x27	UO ₂ 19x19	1.4224	293.15	86.65		1252	A5-12B	0.991768	
UO ₂ 19x19	PuO ₂ -UO ₂ 3x3	1.4224	294.35	83.77		0	A6-6I	0.992139	
PuO ₂ -UO ₂ 19x19	UO ₂ 3x3	1.4224	287.85	81.56		0	A7-1I	1.003014	
UO ₂ 27x27	PuO ₂ -UO ₂ 19x19	1.4224	291.65	92.190	L-shaped UO ₂	1425	A8-10E	0.997889	
UO ₂ 19x19	PuO ₂ -UO ₂ 11x11	1.4224	288.15	92.070	w/ Al Plate	0	A9-9C	0.992159	
UO ₂ 21x21	PuO ₂ -UO ₂ 11x11	1.4224	288.65	73.550	w/ control rods	0	A10-9F	0.986240	
UO ₂ 27x27	PuO ₂ -UO ₂ 19x19	1.4224	291.15	99.800	w/ water slot	1453	A11-10C	0.999570	
UO ₂ 27x27	PuO ₂ -UO ₂ 19x19	1.4224	290.95	106.35	w/ Al Plate	1453	A12-10D	1.001523	

Table 6: Void Effects on Plutonium Critical Experiments

Core configuration	Lattice pitch (cm)	Temperature (°K)	Water height (cm)	Additional feature	Case Number	K_eff (2D)	Comments
23x23	1.3208	292.65	76.011	No Voids	13F2	0.997806	
23x23	1.3208	292.65	96.670	8x8 Voids	13F3	1.006993	
25x23	1.3208	292.05	75.780	8x8 Voids	13F4	1.006604	
25x23	1.3208	292.05	93.890	12x12 Voids	13F5	1.013908	
25x23	1.3208	292.95	75.443	72 Voids	13F6	1.036808	X
25x24	1.3208	292.15	94.984	276 Voids	13F7	1.069501	X
25x24	1.3208	292.05	78.912	153 Voids	13F8	1.056094	X
25x24	1.3208	292.05	70.657	91 Voids	13F9	1.045044	X
25x24	1.3208	292.05	58.952	No Voids	13F10	0.987521	
23x23	1.3208	292.75	75.660	Offset CleanCore	13F11	0.997374	
23x23	1.3208	292.65	79.830	4x4 Offset Voids	13F12	0.999362	
23x23	1.3208	292.75	79.550	4x4 Offset Voids	13F13	0.999131	
23x23	1.3208	293.05	78.870	4x4 Offset Voids	13F14	0.998516	
23x23	1.3208	292.75	77.940	4x4 Offset Voids	13F15	0.997851	
UO ₂ 29x29 PuO ₂ -UO ₂ 23x23	1.3208	292.75	77.520	4x4 Centered Voids 929 ppm Boron	13F16	0.998029	
UO ₂ 29x29 PuO ₂ -UO ₂ 23x23	1.3208	292.95	86.460	8x8 Centered Voids	13F17	1.076313	X

4.2 Analysis of the Effective Neutron Multiplication Factors

Once the 65 core configurations had been calculated, the neutron multiplication factors were used to uncover trends about the methodology and cross section data employed in the DIF3D and WIMS-D4M codes.

Firstly, the criticality calculations for cores containing dispersed void tubes were not adequate under the WIMS-D4M and DIF3D model employed. For cases when only two void tubes surrounded each fuel rod, the average k_{eff} was a totally inadequate value of 1.05186 and the standard deviation was 0.01226, for which the latter was defined as

$$\sigma_* = \sqrt{\frac{\sum_{i=1}^{N^*} (k_i - \bar{k})^2}{N^*}} \quad (1)$$

where asterisk (*) stands for certain sub-category of experiments, *e.g.* experiments with void tubes, multiregion, regular rod pitch, etc.; N^* is the total number of experiments in such a sub-category. The large discrepancy for these cases needs further investigation.

The homogenized nuclear parameters for cells containing fuel rods and perturbing elements were calculated with a MULTICELL model and the probabilities (PCELL) of neutrons traveling among different regions of the cell were predicted using an *adjacent surface ratio*. This methodology provides good results for cases when a fuel rod is surrounded by four void tubes, and also with most other kinds of perturbing elements in the core. However, when a fuel rod is surrounded by two void tubes and two water regions, the adjacent surface ratio rule is not accurate for calculating the PCELL parameters. This problem was not solved in this report and its

solution involves improving the WIMS-D4M homogenization process which is limited by a one-dimensional transport calculation. Therefore, the four (4) cases including two void tubes were eliminated from the k_{eff} -effective averaging process (marked with an "x" in Table 6).

On the other hand, experimental configuration 13F17 (marked with an "x" in Table 6 was also eliminated from the averaging process since a discrepancy was found between the void tube pitch reported in a table and in a corresponding figure in Taylor (1965).

Secondly, a modeling problem was found that prevents successful convergence of the WIMS-D4M SUPERCELL jobs when the fuel rod pitch is greater than 2.5 cm (H/U+Pu ratio ~ 30). Both the DSN and PERSEUS transport solution methods diverged for the SUPERCELL model and a PINCELL model had to be used instead. The average k_{eff} -effective for this case was 1.0257 for two experiments with a fuel rod pitch of 2.6416 cm. These (2) configurations (also marked with an "x" in Table 4) were also eliminated from the averaging process. Figure 7 shows the calculated k_{eff} 's tendency to increase as a function of the fuel rod pitch for both fuel types. The slopes from a linear least squares fit are $0.0009 \Delta k/\text{mm}$ of pitch and $0.0022 \Delta k/\text{mm}$ of pitch, for uranium and MOX fuel types respectively.

The total number of usable core configurations calculated was therefore 58. For 37 of these experiments, the rod-pitch-to-pellet-diameter ratio was comparable to that of a typical PWR assembly (~ 1.5). Table 7 presents the statistical results summary of the SAXTON critical simulations.

Table 7: Analysis of Calculated K-effectives

<u>Classification</u>			Average k- effective	Standard deviation
New Grand Total (Grand Total)	58 experiments (65 experiments)		0.99775 (1.00315)	0.00849 (0.01854)
Fuel rod pitch, (H/U; H/U+Pu), Number of experiments	1.3208 cm (4.45; 4.93), 15		0.99929	0.00692
	1.4224 cm (5.73: 6.35), 37		0.99528	0.00729
	1.8669 cm (NA; 13.79), 2		1.01462	0.00496
	2.0117 cm (15.04; 16.65), 4		1.00641	0.00889
	2.6416 cm (NA; 31.56), 2		1.02572	0.00187
Fuel type	Multiregion		0.99565	0.00455
	UO ₂		0.99185	0.00665
	PuO ₂ -UO ₂	Clean core. Regular rod Pitch (1.4224 cm).	0.99673	0.00768
		Clean core	1.00265	0.01024
		Clean core and borated water	1.00227	0.00901
Perturbing elements	Borated water	Single region	1.00139	0.00497
		Multiregion	0.99750	0.00305
	Water slot		0.99793	0.00452
	Aluminum plate		0.99441	0.00549
	Control rods (Ag-In-Cd)		0.98492	0.00460
	Void tubes	All	1.01403	0.02431
		4 surrounding tubes	1.00255	0.00554
		2 surrounding tubes	1.05186	0.01227

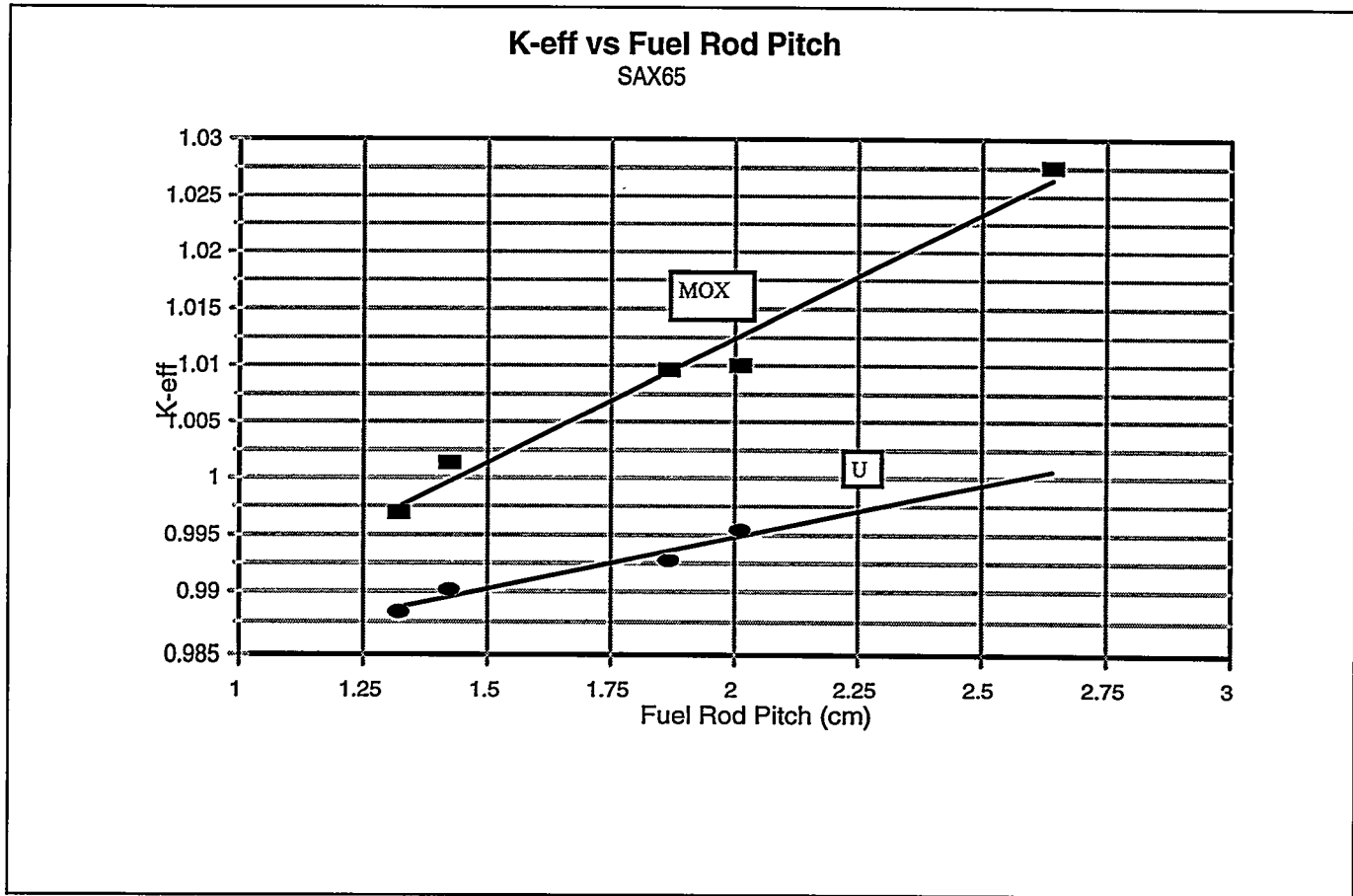


Figure 7: Multiplication Factor as a Function of Fuel Rod Pitch

4.3 Power Distributions

The experimental rod powers were determined by measurement on each rod after the reactor was shut down. Then, each rod power was normalized to a selected rod value with the same type of fuel. The differences in fission product yields from these two fuel rod types posed the problem of calculating the power sharing between them and a experimental method to estimate it. A direct gamma activity and thermal power measurements were carried out by the researchers who observed a difference of approximately 6% immediately after shutdown and a peak difference of 30% four hours later (again after the reactor shutdown). In Taylor (1965), particularly Appendix D, the time-dependent correlation between those

measurements is discussed and a technique was proposed which was also used to estimate the effect of the gap between fuel and clad on the heat production. The effect of the fuel rod manufacture was also addressed (the experiments utilized both pelletized and vibratory compacted MOX fuel). An overall uncertainty estimation of the time-dependent correlation is not provided but an estimated of around 2% is mentioned when the fuel manufacture effect on thermal power was taken into account.

The power sharing problem was not addressed in this analysis due in part to the fact that the computational uncertainty may be on the order of the experimental one. For instance, in the current simulation, the calculated reaction rates (and therefore an estimation of the flux distribution) were

compared with the experimental values for different points around the edge of the core and they were not adequate (underpredicted) for several percent.

Therefore, this analysis has focused first on improving the calculated rod powers (either by improving the flux spectrum or increasing the number of energy groups and/or reducing the mesh size) and comparing the improved values for the selected rods of the same fuel type.

Power maps for selected configurations were compared with the experimental values. Two single region cores with MOX fuel and four multiregion cores (27 x 27 fuel rods) were used to demonstrate typical rod power deviations, defined as experimental minus calculated values. The single region experiments include a water slot and an aluminum plate as criticality perturbing elements and two of the multiregion cores include borated water.

The quarter core layout of these six experiments is presented in Figures 8-13. The neutron multiplication factors are presented for both SUPERCELL and MULTICELL models. K-effective values are different than

the ones presented in Tables 4 and 5 due to a higher number of energy groups employed for these calculations (20 energy groups with a finer partition in the thermal energy range).

The bold value in each rod location represents the experimental relative rod power (relative to a selected rod which was used as a standard) and the smaller number below is the calculated deviation (%).

The average rod power deviation for rods facing the water slot was around 5% (Figure 8). However, for rods facing the aluminum plate, it was below 3% (Figure 9). When five control rods were placed at the center of the reactor core a value of 5.6% as a maximum deviation for the uranium fuel rods was observed. A corresponding deviation of 8.5% was observed for the MOX fuel rods. On the other hand, from the multiregion cases, rod powers were reasonably approximated by the experiment when the core has a moderate size (Figures 10 and 11, square arrays of 19 x 19 fuel rods), or when a nonzero concentration of boron was included in the moderator (Figures 12 and 13). However, for cores with MOX fuel rods near the edge, a larger deviation was observed (Figure 11).

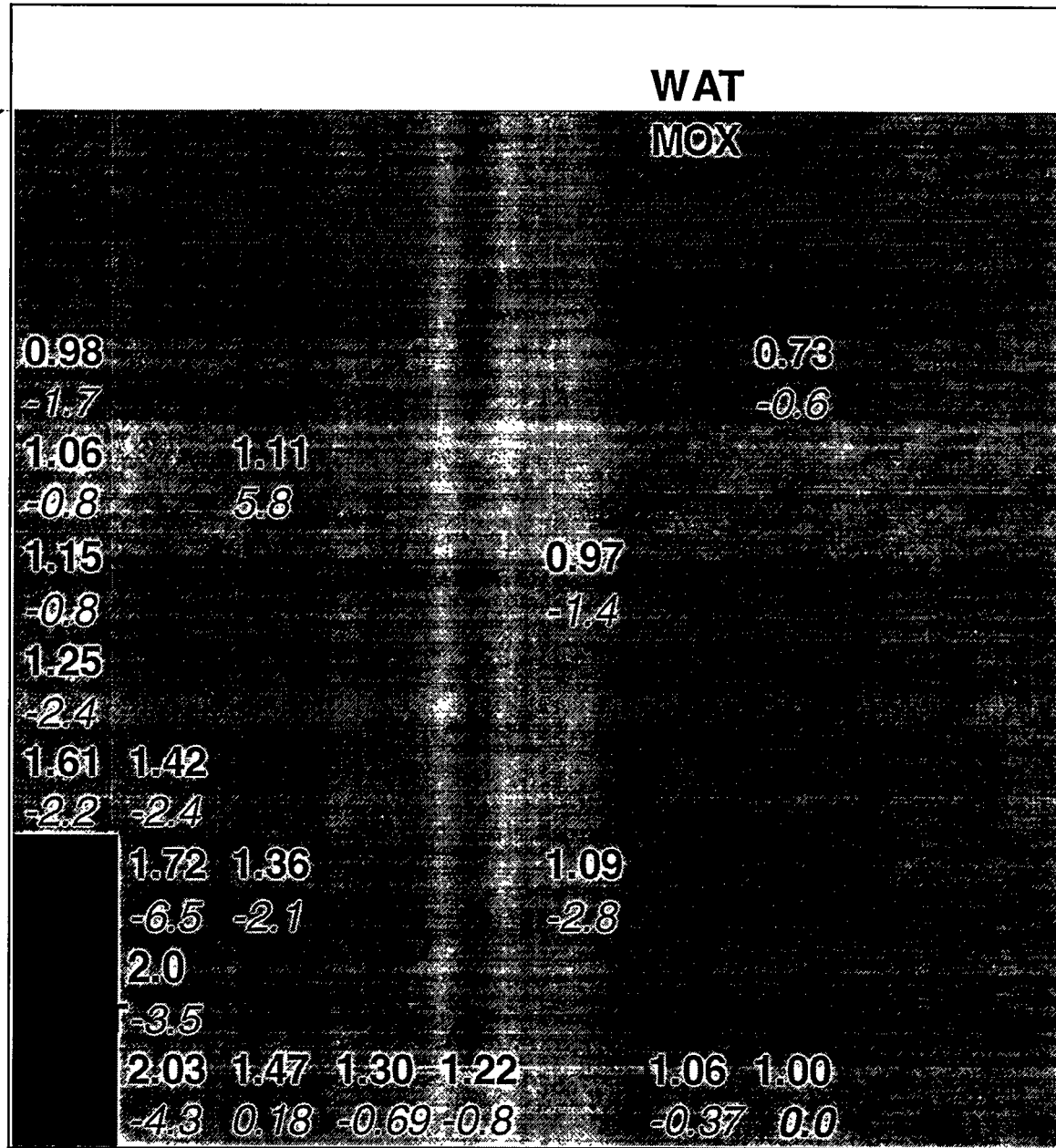


Figure 8: MOX Core with Water Slot
 $k_{\text{eff}} = 1.00517$. Cross sections from WIMS-D4M SUPERCELL model.

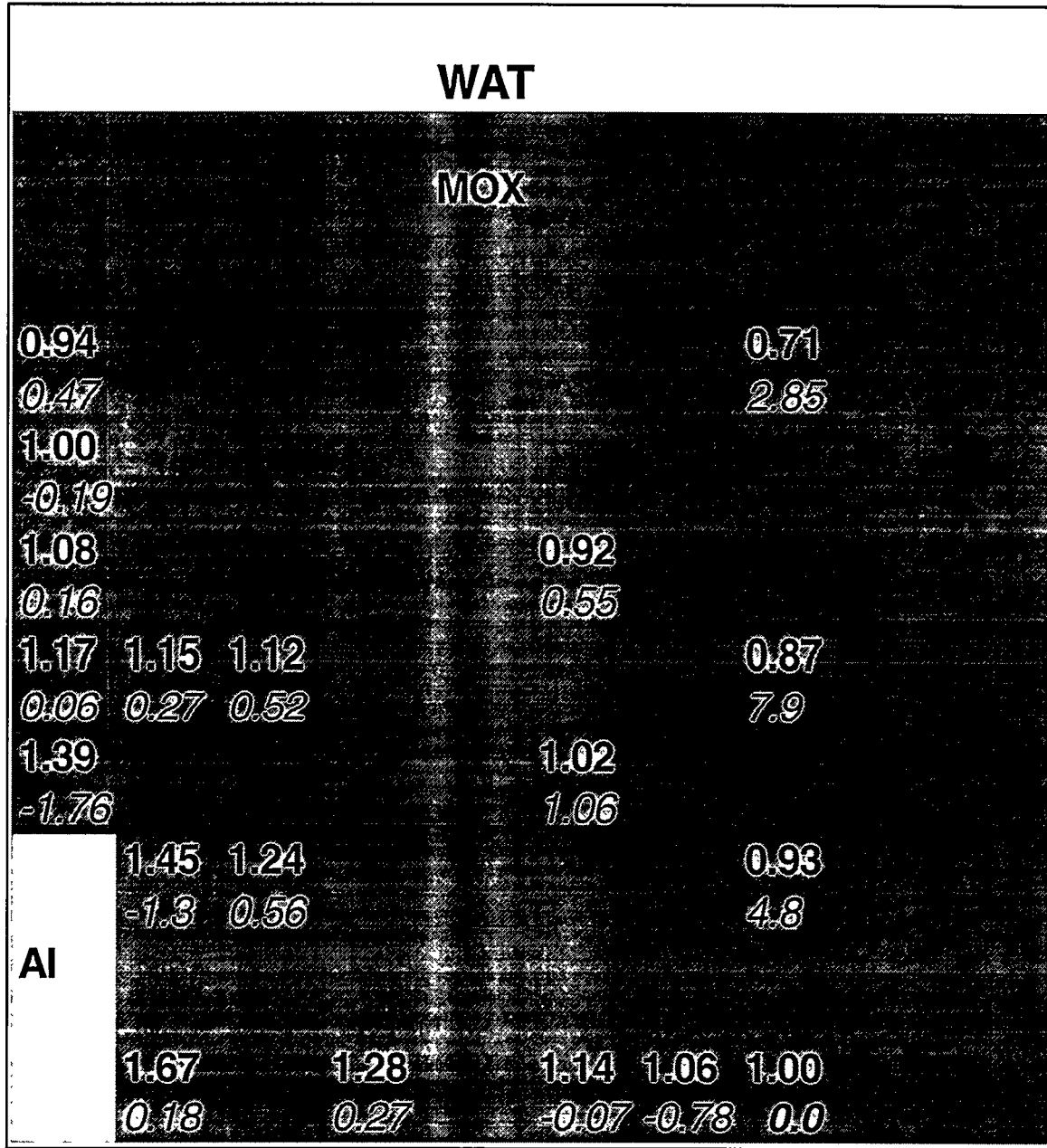


Figure 9: MOX Core with Aluminum Plate
 k-eff = 1.00513. Cross sections from WIMS-D4M SUPERCELL model.

WAT				
1.52	1.46	1.3		1.29
-1.6	-0.04	-1.27		-1.0
1.09	1.05	0.97	0.86	0.8
1.6	0.43	0.66	0.67	1.09
1.04				0.79
1.87				0.79
1.00	0.98		0.87	
0.0	1.28		1.11	
0.95		0.92	0.89	
0.06		1.91	1.14	
0.92	0.9	0.85		
0.05	0.16	0.79		
0.96	0.95	0.91		
1.7	1.41	1.29		
0.97	0.94			
-0.2	-1.02		MOX	UO2
0.99	0.98			
-0.12	0.01			
1.00		0.94	1.00	
0.0		-1.08	0.72	

Figure 10: Multiregion Core: 19x19 Fuel Rods; MOX Fuel Interior (11x11 rods).

k-eff = 1.00169. Cross sections from WIMS-D4M SUPERCELL model

k-eff = 1.00012. Cross sections from WIMS-D4M MULTICELL model

WAT

1.24	1.18	1.09	1.14
-7.4	-6.8	-4.8	-5.3
0.8	0.8	0.74	0.63
-4.17	-1.83	-1.91	-4.7
0.81	0.77	0.7	0.58
2.4	-2.28	-1.58	-2.72
1.00	0.97	0.88	0.7
0.0	-0.4	-1.77	-2.7
0.77	0.5	0.6	
1.67	0.5	0.61	
0.87	0.85	0.77	
-0.15	-0.37	0.94	
0.94	0.93	0.88	
0.49	-0.22	0.6	
0.98	0.95		
1.07	0.25		UO2
0.99	0.98		MOX
-0.21	-0.7		
1.00	0.98		
0.0	1.07		

Figure 11: Multiregion core: 19x19 fuel rods; Uranium fuel interior (11x11 rods).

k-eff = 0.99761. Cross sections from WIMS-D4M SUPERCELL model.

k-eff = 0.99891. Cross sections from WIMS-D4M MULTICELL model.

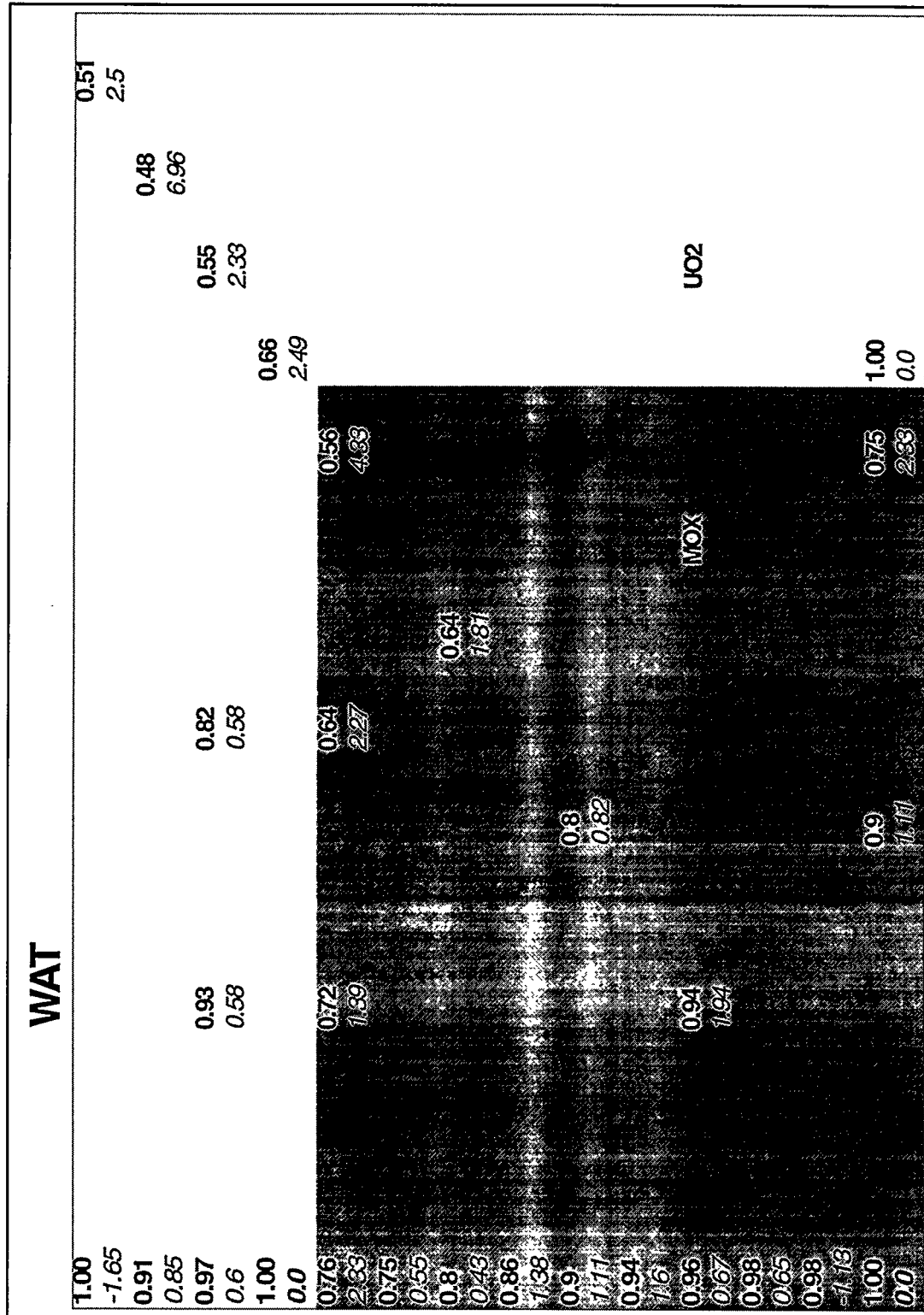


Figure 12: Multiregion Core: 27x27 Fuel Rods; MOX fuel interior (19x19 Rods); 1453 ppm B
 $k_{-eff} = 1.00098$. Cross sections from WIMS-D4M SUPERCELL model.
 $k_{-eff} = 0.99993$. Cross sections from WIMS-D4M MULTICELL model.

WAT

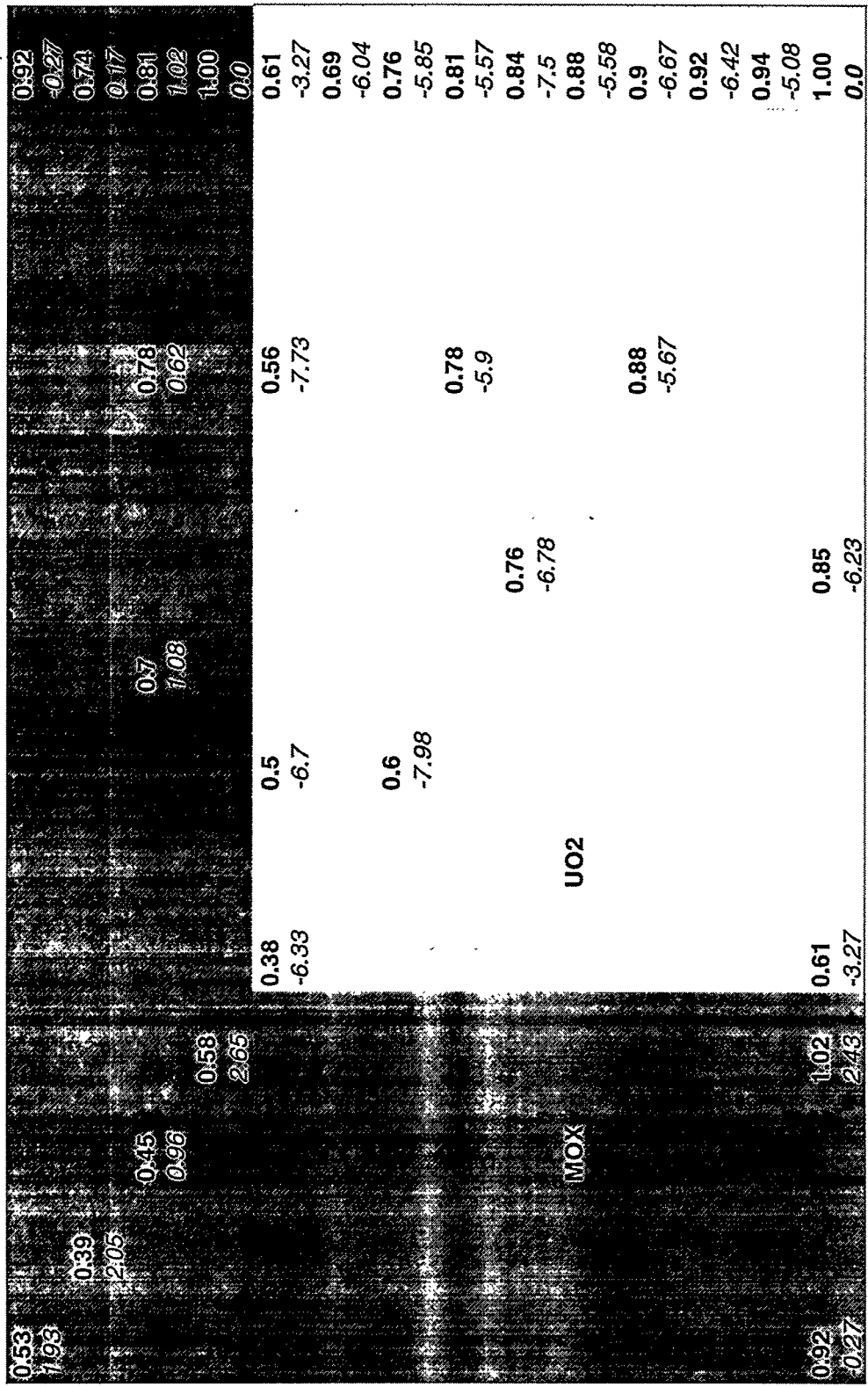


Figure 13: Multiregion Core: 27x27 Fuel Rods; Uranium Fuel Interior (19x19 Rods); 1252 ppm B
 k-eff = 0.99367. Cross sections from WIMS-D4M SUPERCELL model.
 k-eff = 0.99054. Cross sections from WIMS-D4M MULTICELL model.

5. CONCLUSIONS

The aim of the analyses performed here was to produce a quantitative evaluation to allow assessment of the accuracy of the codes WIMS-D4M and DIF3D for MOX fuel related calculations. Under this scope, this report showed the capabilities of these codes and demonstrated a satisfactory simulation of many different experiments. For most of them, the criticality calculations satisfactorily approximated the experimental measurements.

Calculational biases were discussed in this report, *e.g.*, increasing calculated $k_{\text{effective}}$ with rod pitch for experimentally critical configurations. The rod power distributions provided a way to quantify the methodology capabilities in presence of perturbing elements. However, the limitation of the calculational model also prevented good agreement with the measured flux distributions. In general, the fluxes were

under-estimated by the codes. Furthermore, some rod power values on the edge of core, and in front of strongly perturbing elements, were not adequately simulated. Even though this situation is evident, the calculations provided a way of assessing the differences in the numerical simulation of experiments using MOX fuel.

It is also worth noting that some findings (*e.g.*, the $k_{\text{effective}}$ dependence on the fuel rod pitch) was corroborated with results obtained by researchers that used a Monte Carlo methodology (Radulescu and Carron, 1997).

Finally, in this study the importance of the nuclear library, transport routine solver, cell model, energy partition, mesh size, spectra analysis, applicability of diffusion approximation, etc., was assessed and each factor range of applicability explored, confirming a methodology that can be used as a base for future studies on MOX fuel behavior.

REFERENCES

1. “*SAXTON Plutonium Program: Critical Experiments for the SAXTON Partial Plutonium Core*,” E. G. Taylor, December 1965, Westinghouse Electric Corporation.
2. “*WIMS-D4M User Manual: Rev. 0*,” J.R. Deen, W. L. Woodruff and C.I. Costescu, Argonne National Laboratory and University of Illinois, July 1995.
3. “*DIF3D: A Code to Solve One-, Two- and Three-Dimensional Finite Difference Diffusion Theory Problems*,” K.L. Derstine, ANL-82-64, Argonne National Laboratory (1984).
4. “*Evaluation of Critical Experiments Performed at the WREC-CRX Facility (1965)*,” Saxton Plutonium Program, G. Radulescu and I. Carron, University of Texas and Texas A&M University, Revision 2.0 Draft, March 1997.